

η^1 -Coordination of Phosphinine C_5H_5P and Arsenine C_5H_5As to Ruthenium(II) and Osmium(II)^[‡]

Christoph Elschenbroich,^{*,[a]} Jörg Six,^[a] Klaus Harms,^[a] Gernot Frenking,^[a] and Greta Heydenrych^[a]

Keywords: Ru^{II} complex / Os^{II} complex / Phosphinine ligand / Arsenine ligand / X-ray diffraction / Density functional calculations

Reductive complexation of $RuCl_3$ and $OsCl_3$ in the presence of phosphinine C_5H_5P and arsenine C_5H_5As yields the species $trans-Cl_2(\eta^1-C_5H_5E)_4M^{II}$ ($M = Ru, E = P, As; M = Os, E = P$). $trans-Cl_2(\eta^1-C_5H_5As)_4Ru$ constitutes the first arsenine complex of a late transition metal. Further reduction and isolation of the binary complexes $(C_5H_5E)_nM^0$ ($n = 2, 4, 5$) failed, presumably because of metal–ligand bond cleavage. According to X-ray diffraction analysis, $trans-Cl_2(\eta^1-C_5H_5P)_4Ru$ (**3**) features two pairs of coplanar *trans*-phosphinine ligands,

which adopt eclipsed and staggered orientations, respectively, with regard to the $Cl-Ru-Cl$ backbone. DFT calculations indicate a flat curvature of the potential governing conformational change and predict a structure for **3** that differs from that observed in the crystal. This illustrates the need to include intermolecular $Ru-Cl\cdots H$ hydrogen bonding as a structural director.

(© Wiley-VCH Verlag GmbH & Co. KGaA, 69451 Weinheim, Germany, 2008)

Introduction

The group 15 heteroarenes – phosphinine C_5H_5P , in particular – excel in the variability of their coordination modes.^[1,2] However, whereas certain trends have emerged, reliable predictions with regard to the preference for η^1 - or η^6 -coordination as a function of the nature of E (N, P, As) or that of the central metal atom are not yet possible. This is exemplified by the group 8 metals – iron, ruthenium, and osmium with phosphinine and its derivatives were shown to form η^1 - as well as η^6 -coordination complexes,^[3] not to mention more complicated variants.^[1] The problem of reaching reliable generalizations of predictive value is aggravated by the strongly differing experimental conditions of heteroarene–metal complex synthesis; metal–atom ligand–vapor cocondensation is expected to favor products of kinetic control, whereas reductive complexation is prone to yield products of thermodynamic control.

In our work, whenever possible, we have studied the behavior of the parent heteroarenes in order to probe their inherent predilection for a certain coordination mode in binary complexes, unaffected by steric or electronic substituent effects.^[4] This report deals with the reductive complexation of ruthenium trichloride and osmium trichloride in the presence of phosphinine and arsenine, with the aim to

synthesize heavier homologs of $(\eta^1-C_5H_5P)_5Fe$.^[4f] It should be mentioned, however, that in the case of the homocyclic arenes, benzene, mesitylene, and hexamethylbenzene, as ligands, reductive complexation of $RuCl_3$ and $OsCl_3$ led to the 18VE dications $[(\eta^6-Arene)_2M]^{2+}$.^[5] In view of the proven η^6 -ligating property of phosphinine and arsenine^[4c,4h] a similar outcome, i.e. the formation of $[(\eta^6-phosphinine)_2Ru,Os]^{2+}$, could not be excluded a priori. The homoleptic dication $[(2,2'-diphosphinine)_3Ru]^{2+}$, in which η^1 -phosphinine coordination is encountered, has as yet escaped isolation and full characterization because of exceedingly high sensitivity to moisture or nucleophilic reagents.^[2d] Yet, considering the pivotal role derivatives of $[(bpy)_3Ru]^{2+}$ play as sensitizers in solar energy conversion^[6] and the superb electron acceptor character of phosphinines, an examination of the C_5H_5P/Ru^{2+} system seemed warranted. Although of potential interest in homogeneous catalysis,^[7] ruthenium and osmium complexes of monophosphinines are still very rare and those of arsenine are unknown.^[2e]

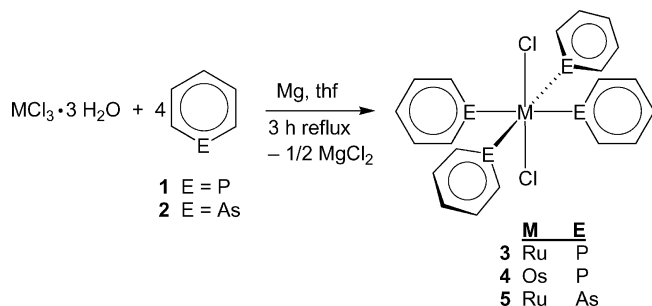
Results and Discussion

Reduction of ruthenium- or osmium trichloride with magnesium in the presence of phosphinine (**1**) afforded *trans*-dichloridotetra(η^1 -phosphinine)ruthenium (**3**) and its osmium congener (**4**), respectively (Scheme 1). In order to explore the effect of a change of E in the heteroarene C_5H_5E on its coordination mode, the combination $RuCl_3$ /arsenine (**2**) was also probed; the analogous product *trans*-

[‡] Metal Complexes of Heteroarenes, 13. Part 12: Ref.^[1]

[a] Fachbereich Chemie der Philipps-Universität Marburg, 35032 Marburg, Germany
Fax: +49-(0)6421-2825653
E-mail: eb@chemie.uni-marburg.de

dichloridotetra(η^1 -arsenine)ruthenium was obtained. Use of **1** and **2** in a lower stoichiometric ratio afforded the same products **3–5** albeit in lower yields; no evidence for bis- η^6 -coordination was seen..



Scheme 1.

Given the high reactivity of their free ligands **1** and **2**, the new complexes **3–5** are surprisingly stable against air and moisture. As solids they can even be handled under ambient conditions for short periods of time. Further reduction by means of stronger reducing agents like sodium/naphthalene failed. Conceivably, **3** undergoes ligand-centered reduction and consecutive metal–ligand bond cleavage [$E_{1/2}(\text{C}_5\text{H}_5\text{P}^{0/-}) = -2.25 \text{ V vs. SCE}$].^[4e]

The structure of **3** as determined by X-ray diffraction is depicted in Figure 1, and bond lengths and angles are col-

lected in Table 1. Prominent features are the *trans* disposition of the chlorido ligands and the coplanarity of the *trans*-positioned, $\sigma(\eta^1)$ -coordinated phosphinine pairs containing the atoms P1, P1a and P7, P7a, respectively. The conformations of these ring planes with regard to the central Cl–Ru–Cl vector are staggered for the phosphinine ligands P1/P1a but eclipsed for the phosphinines P7/P7a. Therefore, the idealized point group for **3** in the crystal is C_{2h} rather than D_4 (staggered, staggered) or D_{4h} (eclipsed, eclipsed) (see Figure 2 for a pictorial description of the conformations).

Conformations encountered in octahedral group 15 heteroarene complexes are multifarious; they reflect a subtle interplay of metal $\pi \rightarrow$ ligand backbonding, interligand repulsion, and packing effects. In the class of homoleptic (η^1 - $\text{C}_5\text{H}_5\text{E}$)_nM complexes, the dication [$(\eta^1\text{-C}_5\text{H}_5\text{N})_6\text{Fe}$]²⁺ (**6**²⁺)^[8] is exceptional in that three pairs of coplanar *trans*-disposed pyridine ligands are encountered that lie in three perpendicular planes. In the other reported examples (η^1 - $\text{C}_5\text{H}_5\text{P}$)₆Cr (**7**),^[4e] (η^1 - $\text{C}_5\text{H}_5\text{P}$)₆Mo (**8**),^[4g] (η^1 - $\text{C}_5\text{H}_5\text{P}$)₆W (**9**),^[4g] and (η^1 - $\text{C}_5\text{H}_5\text{P}$)₅Fe (**10**),^[4f] the torsional angles θ of *trans*-disposed ligand pairs cover the range $18^\circ < \theta < 86^\circ$. However, the molecules **6–10** are not directly comparable to the less crowded complexes **3–5** under discussion here, as they are fairly crowded species. A suitable reference molecule for the latter is the well-known compound *trans*-Cl₂(η^1 - $\text{C}_5\text{H}_5\text{N}$)₄Ru (**11**).^[9] In **11**, the four pyridine “blades” gener-

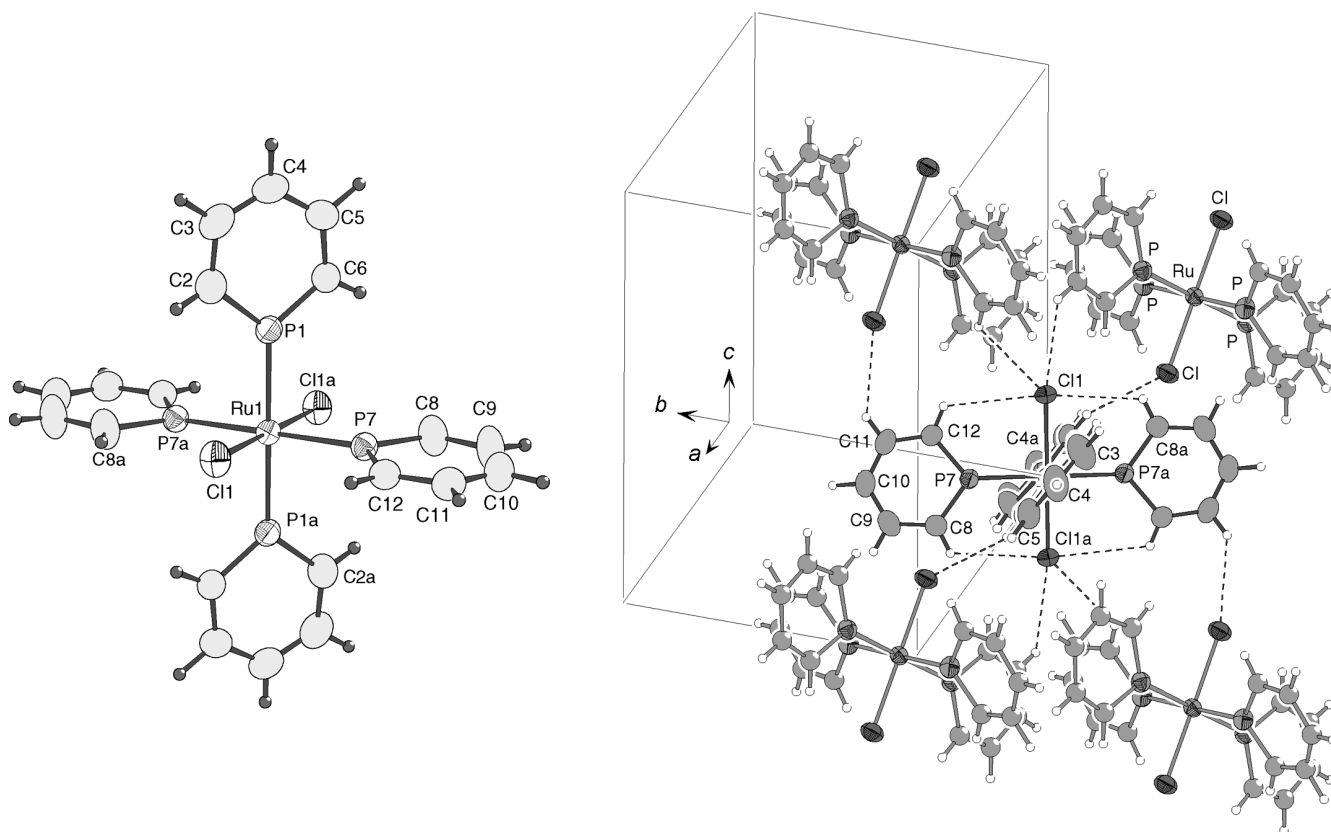


Figure 1. Molecular structure of **3** in the crystal (ORTEP plot, 50% probability ellipsoids). Left: individual molecule and numbering scheme; right: packing diagram. For bond lengths and angles see Table 1.

Table 1. Selected bond lengths [Å] and angles [°] for *trans*-Cl₂(η¹-C₅H₅P)₄Ru (**3**).^[a]

Ru1–P1	2.2967(6)	Ru1–P7	2.3048(6)
P1–C2	1.701(3)	P7–C8	1.697(3)
C2–C3	1.389(4)	C8–C9	1.391(4)
C3–C4	1.369(5)	C9–C10	1.377(4)
C4–C5	1.371(4)	C10–C11	1.371(4)
C5–C6	1.386(4)	C11–C12	1.381(4)
C6–P1	1.696(3)	C12–P7	1.706(2)
C–C _(mean)	1.379		
C–H _(mean)	0.96		
Ru1–Cl1	2.4135(6)		
P1–Ru1–P1a	180.0	P7–Ru1–P7a	180.0
Cl1–Ru1–Cl1a	180.0		
P1–Ru1–Cl1	90.14(2)	P7–Ru1–Cl1	91.08(2)
Cl1–Ru1–P7–C12	5.20(11)		
Cl1–Ru1–P1–C2	−40.76(16)		
C6–P1–C2	103.64(14)	C12–P7–C8	104.07(14)
P1–C2–C3	122.5(3)	P7–C8–C9	122.6(2)
C2–C3–C4	123.8(3)	C8–C9–C10	123.6(3)
C3–C4–C5	123.5(3)	C9–C10–C11	123.2(3)
C4–C5–C6	123.2(3)	C10–C11–C12	124.3(3)
C5–C6–P1	123.2(2)	C11–C12–P7	122.3(2)
(P1,P7,P1a,P7a)–(P1, ... C6)			47.97(6)
(P1,P7,P1a,P7a)–(P7, ... C12)			86.20(5)
Hydrogen bonds			
D–H...A	<i>d</i> (C–H)	<i>d</i> (H...Cl)	<i>d</i> (C...Cl)
C11–H11...Cl1#2	0.93(3)	2.87(3)	3.615(3)
C12–H12...Cl1	0.92(2)	3.04(3)	3.584(3)
C8–H8...Cl1#1	0.91(3)	2.91(3)	3.457(3)
C6–H6...Cl1#3	0.93(3)	2.91(3)	3.533(3)
			<(CHCl)
			137(2)
			119.1(19)
			120(2)
			126(2)

[a] Free ligand **1**:^[2a] P–C2, P–C6 1.73 Å; C2–C3, C5–C6 1.41 Å; C3–C4, C4–C5 1.38 Å; C2–P–C6 101°. Symmetry transformations used to generate equivalent atoms: #1 −*x*, −*y*, −*z*; #2 −*x*, *y* + 1/2, −*z* + 1/2; #3 *x*, −*y* + 1/2, *z* − 1/2.

ate a perfect propeller – the dihedral angle between the plane of the coordinated nitrogen atoms and the pyridine rings is 51°. Contrarily, in the phosphinine analogous complex **3**, the metal–ligand conformations are different in that the coplanar pairs of *trans*-positioned phosphinine ligands feature dihedral angles of 48° (P1, ... C6) and 86° (P7, ... C12) relative to the plane P1, P7, P1a, P7a. It would be difficult to explain this symmetry lowering on going from **11** to **3** in terms of intramolecular electronic effects or *ortho*-hydrogen(ligand)–RuCl repulsion because both $\text{Ru} \rightarrow \text{PC}_5\text{H}_5$ backbonding as well as steric effects should preserve the fourfold symmetry. A hint is provided by an inspection of the packing diagram. In Figure 1 (bottom) intra- and intermolecular H...Cl connections are indicated, which, at least in part, point to weak C–H...Cl hydrogen bonding. The distances *d*(H...Cl) are only marginally smaller than the sum of the van der Waals radii for H and Cl (2.96 Å^[10]). It has been stated, however, that the van der Waals cutoffs as a means of identifying hydrogen bonds may be inappropriate as the comparably low dependence of the distance of the electrostatic forces will cause them to be effective beyond the van der Waals separation.^[11h,11i] Therefore, in cooperation, even weak C–H...Cl hydrogen bonds may well play the role of structural directors in the crystal. C–H...Cl bonding has been controversial for many years but in the last two decades has become generally ac-

cepted.^[11] In this context, it has been concluded that contrary to C–Cl bonds, M–Cl bonds are good hydrogen-bond acceptors, which rival the chloride anion,^[11f] thereby playing an important role in determining the structure of metal complexes.^[11i] Conceivably, the Cl–Ru–Cl backbone engages in very weak intramolecular C–H...Cl hydrogen bonding to the pair of phosphinine ligands, which assume an eclipsed disposition with regard to Cl–Ru–Cl, and in weak intermolecular hydrogen bonding to phosphinine ligand pairs of neighboring complex units. The latter interaction is maximized if these phosphinine pairs adopt a staggered conformation relative to the Cl–Ru–Cl backbone. This could explain the observation that packing in the crystal reduces the symmetry of **3** such that the conformations of the two phosphinine pairs differ radically. Notwithstanding, the two pairs of bond lengths Ru–P1, Ru–P1a and Ru–P7, Ru–P7a are almost identical. Therefore, $\text{Ru} \rightarrow \text{PC}_5\text{H}_5$ backbonding appears to be essentially independent of ClRuCl–phosphinine conformation, and an intramolecular electronic effect as a cause for the shape of **3** in the crystal can be dismissed.

The extent of π bonding can be gauged from a comparison with Ru–P bond lengths in related complexes: RuCl₂(PF₃)₂(PPh₃)₂ (2.17, 2.46 Å),^[12] *trans*-RuCl₂(dppm)₂ (2.34–2.37 Å),^[13] which places the Ru–P distances in the range 2.297–2.305 Å in **3** at the lower end of that for Ru^{II}-organophosphane complexes and yet considerably greater than that for Ru^{II}-PF₃. The fairly short Ru–P bond length in RuCl₂(dmsol)₂(tetramethyldiphosphane) (2.24 Å)^[14] reflects the fact that here π -acceptor ligands in a position *trans* to the diphosphinine binding sites are absent.

As observed previously,^[2,4] the intraphosphinine dimensions in **3** are influenced by η^1 -coordination only to a small extent. Thus, the classical notion of bond lengthening caused by population of the intraligand antibonding π^* MO does not seem to apply here. Rather, as discussed for (η^1 -C₅H₅P)₆M (M = Cr, Mo, W),^[4c,4g] η^1 -coordinated λ_3 -phosphinine may be regarded as an ylidic form in which the positive formal charge resides on the η^1 -P atom and the negative charge is delocalized over the pentadienyl (C2–C6) segment. The observed coordination induced shortening of the P–C2 and P–C6 bonds may then be of electrostatic origin.

Conformational Peculiarity of **3** Studied by DFT Calculations

In order to explore whether the structure of **3** in the crystal is governed by intermolecular forces of the type discussed above or whether there exists an inherent preference for the conformations observed, quantum chemical calculations have been performed for the pyridine complex **11** and the phosphinine complex **3** of analogous composition but with differing conformation in the ligand sphere.

Experimentally, it had been established that the complex Ru(NC₅H₅)₄Cl₂ (**11**) crystallizes in a doubly staggered conformation, whereas the complex Ru(PC₅H₅)₄Cl₂ (**3**) exhibits staggered as well as eclipsed conformations. Inspired by this

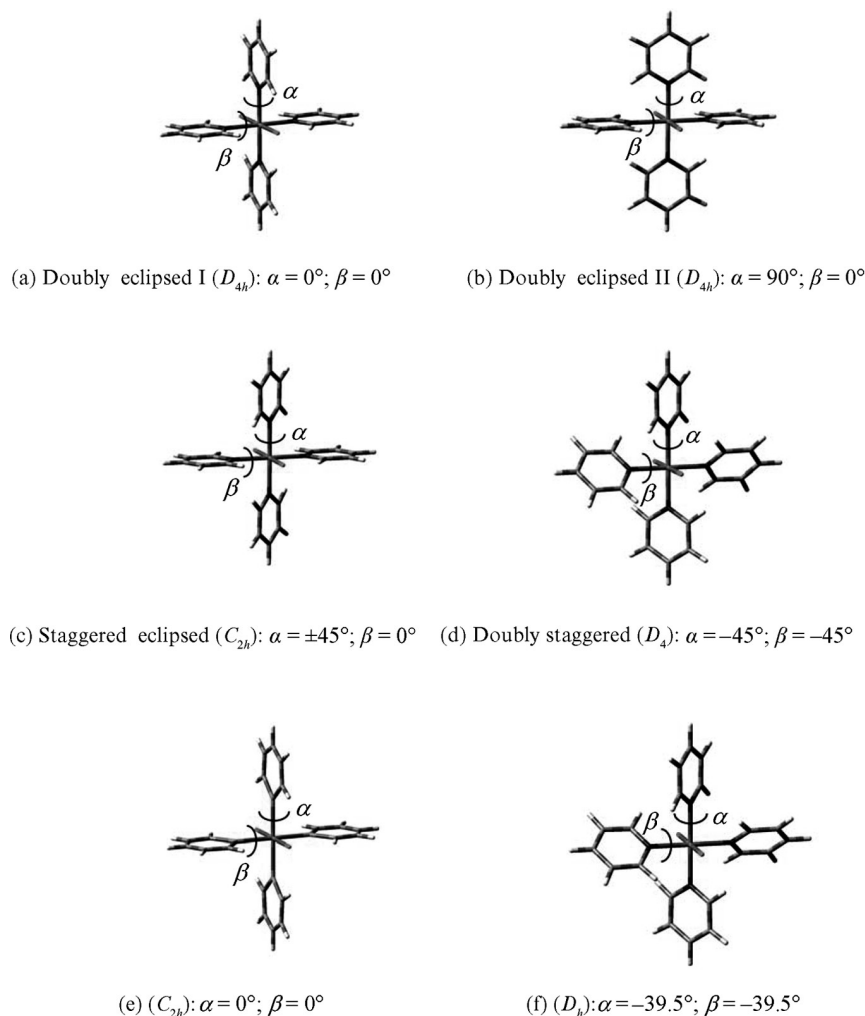


Figure 2. (a–d) Partially optimized geometries for $\text{Ru}(\text{NC}_5\text{H}_5)_4\text{Cl}_2$ (RI-BP86/SVP). The angles α and β shown on the images define the dihedral angle made by the pyridine plane and the C–Cl vector. The partially optimized geometries for the phosphinine complexes have the same α and β values and are not shown here. The values for α and β were frozen at the values shown in the figures, while the remaining geometrical parameters were optimized. (e) Minimum energy (BP86/SVP) structures for $\text{Ru}(\text{PC}_5\text{H}_5)_4\text{Cl}_2$ (doubly eclipsed form I) and (f) for $\text{Ru}(\text{NC}_5\text{H}_5)_4\text{Cl}_2$ (doubly staggered). These structures are the lowest-energy structures obtained by relaxing the idealized geometries in (a–d), and the energies in Table 2 are relative to the energies of these structures.

observation, we chose four idealized conformations and, for both complexes **3** and **11**, performed DFT calculations in which the geometries were frozen in order to retain these conformations. The relevant bond angles are given in Figure 2a–d, and the relative energies are listed in Table 2. Subsequently, we allowed each geometry to relax to the minimum energy structures. The resulting geometries for **3** (Figure 2e) and **11** (Figure 2f) are also shown. Inspection of Table 2 reveals that the calculations correctly assign the minimum energy to the doubly staggered structure of $\text{Ru}(\text{NC}_5\text{H}_5)_4\text{Cl}_2$ (**11**), and alternative conformations lie considerably higher in energy. Contrarily, for $\text{Ru}(\text{PC}_5\text{H}_5)_4\text{Cl}_2$ (**3**), the calculation yields the doubly eclipsed form I as the energetically most favorable conformer for the free molecule. However, the staggered–eclipsed structure prevalent in the crystal of **3** lies a mere $3.6 \text{ kcal mol}^{-1}$ higher in energy. It is noteworthy that the conformational energy profile of the pyridine complex **11** varies considerably more (min.

1.47 , max. $19.95 \text{ kcal mol}^{-1}$) than that of the phosphinine complex **3** (min. 0.44 , max. $7.95 \text{ kcal mol}^{-1}$). This may be traced to a more pronounced *ortho*-H/Ru–Cl repulsion in the eclipsed form of **11** relative to that of **3**, which is caused by the short Ru–N distance. Allowing the molecules to relax to their minimum energy conformations only slightly modifies the structures considered to be the most favorable ones according to Table 2: the doubly staggered form of **11** experiences a variation in the twist angle from 45° to 39.5° and the doubly eclipsed form I remains virtually unchanged. The obvious inconsistency in experiment and calculation for the lowest energy structure of **3** reflects the necessity to include intermolecular interactions as factors contributing to the molecular structure in the solid state; this is particularly relevant in case of the phosphinine complex **3**, for which the potential energy graph for ligand rotation about the Ru–P axis displays a rather flat curvature (Table 2).

Table 2. Relative energies [kcal mol^{−1}] at the RI-BP86/SVP level of theory for each of the four restricted optimizations for both complexes. The energies are relative to the energies obtained for the completely optimized geometries of lowest energy for each complex.

		BP86/SVP
Ru(NC ₅ H ₅) ₂ Cl ₂	Doubly eclipsed I (<i>D</i> _{4h})	10.85
	Doubly eclipsed II (<i>D</i> _{4h})	19.95
	Staggered eclipsed (<i>C</i> _{2h})	9.61
	Doubly staggered (<i>D</i> ₄)	1.47
Ru(PC ₅ H ₅) ₂ Cl ₂	Doubly eclipsed I (<i>D</i> _{4h})	0.44
	Doubly eclipsed II (<i>D</i> _{4h})	7.79
	Staggered eclipsed (<i>C</i> _{2h})	4.01
	Doubly staggered (<i>D</i> ₄)	7.95

NMR Spectroscopy and Cyclic Voltammetry

While crystals suitable for X-ray diffraction could be grown for **3** only, the analytical and NMR spectroscopic data ascertain that the products **4** and **5** possess compositions and structures in solution analogous to those of **3**. ¹H-, ¹³C-, and ³¹P NMR spectroscopic data are collected in Table 3; the spectra of complexes **3–5** are very similar to those of the free ligands, thereby attesting to the σ(η¹)-coordination mode, in which, contrary to η⁶-coordination, the π-electron system of the heterocycles is perturbed to a small extent. The coordination shifts for the complexes (η¹-C₅H₅E)₄MCl₂ [M = Ru^{II}, Os^{II}] are somewhat smaller than those for the homoleptic complexes (η¹-C₅H₅E)_nM (M = Cr, Mo, W, Fe, Ni) since the former contain central metal atoms in a positive oxidation state and are less inclined to engage in metal→ligand backdonation. The most conspicuous trend, which can be gleaned from Table 3, is the very pronounced increase in ³¹P shielding upon varying the central metal atom towards higher transition series. This has been observed previously for binary phosphinine complexes of Cr, Mo, and W and also for phosphane complexes.^[4g]

The redox properties of **3–5** have been evaluated by cyclic voltammetry (Figure 3). Whereas in the cyclic voltammograms of the homoleptic octahedral complexes (η¹-

C₅H₅P)₆M (Cr, Mo, W) the anodic region shows two oxidation steps, which are reversible for M = Cr at scan rates $\nu \geq 100$ mV s^{−1},^[4e,4g] electrochemical oxidation for complexes **3–5** is ill-defined. Reduction of **3** and **4** gives rise to two cathodic waves; the first wave $E_{p,c}(\mathbf{3}) = -1.68$ V, $E_{p,c}(\mathbf{4}) = -1.73$ V involves the respective complex and the second wave $E_{p,c} = -2.22$ V the free ligand phosphinine.^[4e] The small peak currents for reoxidation and the large peak separations indicate irreversible processes. These CV characteristics indicate why chemical reduction of **3** and **4** to M(0)–phosphinine complexes failed. The cyclic voltammogram of the arsenine complex **5** contains only a weak indication for

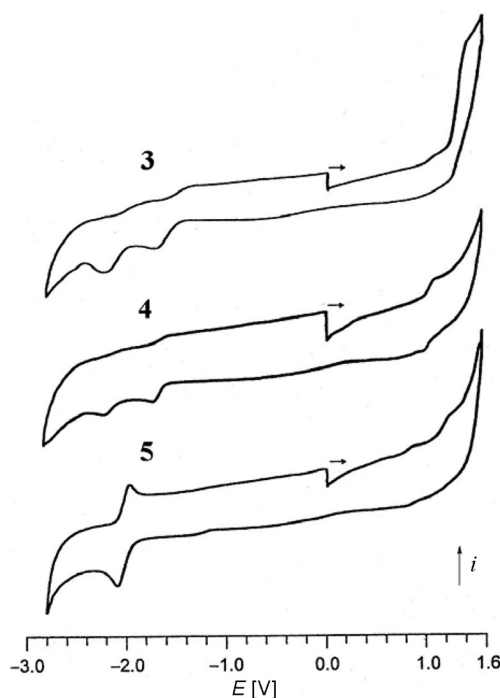


Figure 3. Cyclic voltammetric traces for *trans*-Cl₂(η¹-C₅H₅P)₄Ru (**3**), *trans*-Cl₂(η¹-C₅H₅P)₄Os (**4**), and *trans*-Cl₂(η¹-C₅H₅As)₄Ru (**5**) in dimethoxyethane, *n*-Bu₄NClO₄, *T* = −40 °C, ν = 100 mV s^{−1} vs. SCE. Potential data, see text.

Table 3. ¹H-, ¹³C-, and ³¹P NMR data for the complexes **3–5** and the free ligands **1**^[4g] and **2**^[4h] ([D₈]thf, *T* = 300 K).^[a]

	1 ^[4g]	2	3	5	4
δH _{2,6} (Δδ)	8.77	9.79	8.90 (0.13)	9.98 (0.19)	8.74 (−0.03)
² J _{HP}	38.5		n.r.		n.r.
δH _{3,5} (Δδ)	7.87	7.90	7.84 (−0.03)	7.89 (−0.01)	7.86 (−0.01)
³ J _{HP}	8.1		n.r.		n.r.
δH ₄ (Δδ)	7.55	7.60	7.33 (−0.22)	7.45 (−0.15)	7.29 (−0.26)
⁴ J _{HP}	3.3		n.r.		n.r.
δP (Δδ)	206.5		207.5 (1.0)		159.3 (−47.2)
δC _{2,6} (Δδ)	155.1	168.3	143.7 (−11.4)	157.6 (−10.7)	140.0 (−15.1)
¹ J _{CP}	54.0		n.r.		n.r.
² J _{CM}					15.3
δC _{3,5} (Δδ)	134.7	133.8	138.3 (3.6)	137.6 (3.8)	138.7 (4.0)
² J _{CP}	14.3		n.r.		n.r.
³ J _{CM}					n.r.
δC ₄ (Δδ)	129.8	129.0	126.9 (−2.9)	126.2 (−2.8)	126.6 (−3.2)
³ J _{CP}	22.0		n.r.		n.r.
⁴ J _{CM}					12.9

[a] n.r. = not resolved.

complex reduction at $E_{p,c}(5) \approx -1.30$ V but a reversible wave at $E_{1/2}(2^{0/-}) = -2.08$ for free arsenine. The irreversible nature of the reductions of the η^1 -phosphinine and η^1 -arsenine complexes **3–5** contrasts with the reversibility of the 0/–1 couples for the $(\eta^6\text{-C}_5\text{H}_5\text{P,As})_2\text{M}(0)$ species ($\text{M} = \text{Ti}, \text{V}, \text{Cr}$).^[4h] This can be rationalized in terms of the increased thermodynamic stability of the sandwich complexes in which the heteroarene may be regarded as a chelating ligand as it formally occupies three metal coordination sites. The cyclic voltammogram of **5**, in particular the strongly differing cathodic peak currents for the alleged reduction of complex **5**, and that of the free ligand **2** indicate that **2** was present in high concentration in the test solution as a result of complex dissociation prior to electrochemical measurement. The differing voltammetric behavior of **3** and **5** would then suggest that arsenine **2** is a weaker $\sigma(\eta^1)$ ligand than phosphinine **1**. This is in line with generalizations put forward previously.

In conclusion, reductive complexation of RuCl_3 and OsCl_3 failed to yield the higher homologues of $(\eta^1\text{-C}_5\text{H}_5\text{P})_5\text{-Fe}^{[4f]}$ – reduction beyond the $\text{Ru}^{\text{II}}, \text{Os}^{\text{II}}$ stage effected metal–ligand cleavage. Yet, the ternary complexes of the type $\text{trans-Cl}_2\text{M}(\eta^1\text{-C}_5\text{H}_5\text{E})_4$ ($\text{M} = \text{Ru}, \text{Os}$; $\text{E} = \text{P}, \text{As}$) may serve as potential building blocks for the construction of photoactive molecular assemblies as has been proposed in the past for $\text{trans-}[\text{Ru}(\eta^1\text{-pyridine})_4]^{2+}$ units.^[15]

Experimental Section

Chemical manipulations and physical measurements were performed using techniques and instruments specified previously.^[4e] Phosphinine (**1**)^[16] and arsenine (**2**)^[17] were prepared by literature methods.

trans-Dichloridotetra(η^1 -phosphinine)ruthenium (3): A solution of $\text{RuCl}_3 \cdot 3\text{H}_2\text{O}$ (0.42 mmol) in thf (50 mL) was added dropwise to magnesium powder (383 mg, 15.8 mmol), which previously had been heated to 160 °C for 30 min, and a solution of phosphinine (296 mg, 3.1 mmol) in thf (20 mL). The mixture was heated at reflux for 3 h, whereby the color changed from dark brown to brownish yellow. After removal of the solvent in vacuo, the dark brown residue was taken up in benzene (60 mL), and the solution was filtered through a G4 sintered disk. The yellow filtrate was dried, and the crystalline residue was washed with petroleum ether (10 mL, 40/60) and dried in vacuo. Yield: 219 mg (0.39 mmol, 94%). M.p. 224 °C (decomp.). EI-MS (70 eV): m/z (%) = 96 (100) [$\text{C}_5\text{H}_5\text{P}^+$], 70 (15) [$\text{C}_5\text{H}_5\text{P}^+ - \text{C}_2\text{H}_2$]. UV/Vis (thf, 25 °C): λ_{max} (ϵ , $\text{L mol}^{-1} \text{cm}^{-1}$) = 249 (9000), 255 (8600), 297 (4300), 320 nm (4100). NMR spectroscopic data, see text. $\text{C}_{20}\text{H}_{20}\text{Cl}_2\text{P}_4\text{Ru}$ (556.25): calcd. C 43.19, H 3.62; found C 43.08, H 3.80.

trans-Dichloridotetra(η^1 -phosphinine)osmium (4): The synthesis of **4** proceeded as described for **3** from magnesium powder (414 mg, 17.0 mmol), phosphinine (329 mg, 3.42 mmol) in thf (20 mL) and $\text{OsCl}_3 \cdot 3\text{H}_2\text{O}$ (142 mg, 0.41 mmol) in thf (50 mL). Yield: 203 mg (0.31 mmol, 78%), yellow crystals. M.p. 224 °C (decomp.). EI-MS (70 eV): m/z (%) = 96(100) [$\text{C}_5\text{H}_5\text{P}^+$], 70 (54) [$\text{L}^+ - \text{C}_2\text{H}_2$]. UV/Vis (thf, 25 °C): λ_{max} (ϵ , $\text{L mol}^{-1} \text{cm}^{-1}$) = 249 (8800), 261 (8800), 330 (9100), 389 nm (1800). NMR spectroscopic data, see text. $\text{C}_{20}\text{H}_{20}\text{Cl}_2\text{P}_4\text{Os}$ (645.38): calcd. C 37.22, H 3.12; found C 36.64, H 3.63.

trans-Dichloridotetra(η^1 -arsenine)ruthenium (5): The synthesis proceeds as described for **3** from magnesium powder (401 mg, 16.5 mmol), arsenine (550 mg, 3.93 mmol) in thf (20 mL) and $\text{RuCl}_3 \cdot 3\text{H}_2\text{O}$ (109 mg, 0.42 mmol) in thf (50 mL). Yield: 151 mg (0.21 mmol, 50%), orange microcrystalline material. M.p. 170 °C (decomp.). EI-MS (70 eV): m/z (%) = 140 (100) [$\text{C}_5\text{H}_5\text{As}^+$], 114 (18) [$\text{C}_5\text{H}_5\text{As}^+ - \text{C}_2\text{H}_2$]. UV/Vis (thf, 25 °C): λ_{max} (ϵ , $\text{L mol}^{-1} \text{cm}^{-1}$) = 249 (9900), 267 (12000), 311 (5000), 345 nm (4300). NMR spectroscopic data, see text. $\text{C}_{20}\text{H}_{20}\text{As}_4\text{Cl}_2\text{Ru}$ (732.04): calcd. C 32.82, H 2.75; found C 31.97, H 2.94.

X-ray Crystallographic Study of 3: A single crystal was mounted onto a glass fiber in a drop of inert oil and frozen in the cold nitrogen stream of the cooling device. The diffraction experiment was carried out at 193 K on a STOE IPDS diffractometer by using graphite monochromated Mo-K_α radiation. Cell parameters were obtained from least-squares refinement of 5000 reflections. The structure was solved by direct methods.^[18] Structure refinement was made on F^2 values by the full-matrix least-squares technique.^[19] The weighting scheme suggested by the program was used. All non-hydrogen atoms were refined with anisotropic displacement parameters. The hydrogen atoms were located and refined isotropically. Other experimental details and crystal data are summarized in Table 4. CCDC-640182 contains the supplementary crystallographic data for this paper. These data can be obtained free of charge from The Cambridge Crystallographic Data Centre via www.ccdc.cam.ac.uk/data_request/cif.

Table 4. Crystallographic data for **3**.

Empirical formula	$\text{C}_{20}\text{H}_{20}\text{Cl}_2\text{P}_4\text{Ru}$
F_w	556.21
Crystal system	monoclinic
Space group	$P2_1/c$
a [Å]	9.4483(8)
b [Å]	9.5826(8)
c [Å]	13.1101(11)
β [°]	104.473(7)
Z	2
V [Å ³]	1149.31(17)
D_{calcd} [Mg m^{-3}]	1.607
μ [mm^{-1}]	1.197
$F(000)$	556
crystal size [mm]	$0.35 \times 0.18 \times 0.15$
θ range [°]	2.66–25.54
index ranges	$h -11/11, k -11/11, l -15/15$
no. of reflections collected	11435
no. of independent reflections	2104 [$R(\text{int}) = 0.0406$]
no. of observed reflections	1897 [$I > 2\sigma(I)$]
no. of reflections used for refinement	2104
largest diff. peak and hole [e Å^{-3}]	0.313 and –0.277
goodness-of-fit on F^2	1.131
wR_2 (all data)	0.0517
R_1 (observed data)	0.0189

Computational Details: All geometries were optimized at the RI-BP86/SVP level of theory [BP86 denotes the generalized gradient approximation (GGA) to density functional theory (DFT) using the exchange functional of Becke^[20] in conjunction with the correlation functional of Perdew^[21,22] employing Gaussian03.^[23] Quasi-relativistic ECPs have been used for As and Ru,^[24a] while all-electron SVP basis sets were used for the other atoms.^[24b] Subsequently, the nature of the stationary points were characterized by calculating the Hessian matrix at the stationary points analytically. All structures optimized without any constraints were found to be minima.

Acknowledgments

This work was supported by the Deutsche Forschungsgemeinschaft (Grant El 62/7-3). G. H. thanks the National Research Foundation of South Africa (Grant number SFP2005110900004) and the DAAD of Germany (Grant number A/05/52686) for post-doctoral funding.

- [1] C. Elschenbroich, J. Six, K. Harms, *Chem. Commun.* **2006**, 3429–3431.
- [2] a) A. J. Ashe III, *Acc. Chem. Res.* **1978**, *11*, 153–157; b) P. LeFloch, F. Mathey, *Coord. Chem. Rev.* **1998**, *178–180*, 771–791; c) N. Mézailles, F. Mathey, P. LeFloch, *Prog. Inorg. Chem.* **2001**, *49*, 455–550; d) P. LeFloch, *Coord. Chem. Rev.* **2006**, *250*, 627–681; e) A. P. Sadimenko, *Adv. Heterocycl. Chem.* **2005**, *89*, 125–157.
- [3] a) P. LeFloch, F. Knoch, F. Kremer, F. Mathey, J. Scholz, K.-H. Thiele, U. Zenneck, *Eur. J. Inorg. Chem.* **1998**, 119–126; b) N. Mézailles, L. Ricard, F. Mathey, P. LeFloch, *Organometallics* **2001**, *20*, 3304–3307.
- [4] a) C. Elschenbroich, J. Kroker, W. Massa, M. Wünsch, A. J. Ashe III, *Angew. Chem. Int. Ed. Engl.* **1986**, *25*, 571–572; b) C. Elschenbroich, J. Koch, J. Kroker, M. Wünsch, W. Massa, G. Baum, *Chem. Ber.* **1988**, *121*, 1983–1988; c) C. Elschenbroich, M. Nowotny, B. Metz, W. Massa, J. Graulich, K. Biehler, J. Sauer, *Angew. Chem. Int. Ed. Engl.* **1991**, *30*, 547–550; d) C. Elschenbroich, M. Nowotny, A. Behrendt, W. Massa, S. Wocadlo, *Angew. Chem. Int. Ed. Engl.* **1992**, *31*, 1343–1345; e) C. Elschenbroich, M. Nowotny, J. Kroker, A. Behrendt, W. Massa, S. Wocadlo, *J. Organomet. Chem.* **1993**, *459*, 157–167; f) C. Elschenbroich, M. Nowotny, A. Behrendt, K. Harms, S. Wocadlo, J. Pebler, *J. Am. Chem. Soc.* **1994**, *116*, 6217–6219; g) C. Elschenbroich, S. Voss, O. Schiemann, A. Lippek, K. Harms, *Organometallics* **1998**, *17*, 4417–4424; h) C. Elschenbroich, J. Kroker, M. Nowotny, A. Behrendt, B. Metz, K. Harms, *Organometallics* **1999**, *18*, 1495–1503.
- [5] a) E. O. Fischer, R. Böttcher, *Z. Anorg. Allg. Chem.* **1957**, *291*, 305–309; b) D. Jones, L. Pratt, G. Wilkinson, *J. Chem. Soc.* **1962**, 4458–4463; c) E. O. Fischer, C. Elschenbroich, *Chem. Ber.* **1970**, *103*, 162–172; d) P. J. Domaille, S. D. Ittel, J. P. Jesson, D. A. Schweigart, *J. Organomet. Chem.* **1980**, *202*, 191–199.
- [6] M. K. Nazeeruddin, M. Grätzel, *Comprehensive Coord. Chem.* **2004**, *9*, 719–758.
- [7] a) B. Breit, *Chem. Commun.* **1996**, 2071–2072; b) B. Breit, R. Winde, K. Harms, *J. Chem. Soc. Perkin Trans. 1* **1997**, 2681–2682.
- [8] a) W. Hieber, R. Werner, *Chem. Ber.* **1957**, *90*, 286–296; b) W. Hieber, R. Werner, *Chem. Ber.* **1957**, *90*, 1116–1120; c) R. J. Doedens, L. F. Dahl, *J. Am. Chem. Soc.* **1966**, *88*, 4847–4855.
- [9] a) W.-T. Wong, T.-C. Lau, *Acta Crystallogr., Sect. C* **1994**, *50*, 1406–1407; M. R. J. Elsegood, D. A. Tocher, *Acta Crystallogr., Sect. C* **1995**, *51*, 40–42.
- [10] A. Bondi, *J. Phys. Chem.* **1964**, *68*, 441–451.
- [11] a) R. Glasstone, *Trans. Faraday Soc.* **1937**, *33*, 200–206; b) J. Donohue in *Structural Chemistry and Molecular Biology* (Eds.: A. Rich, N. Davidson, W. H. Freeman), San Francisco, CA, **1968**; c) R. Taylor, O. Kennard, *J. Am. Chem. Soc.* **1982**, *104*, 5063–5070; d) G. P. A. Yap, A. L. Rheingold, P. Das, R. H. Crabtree, *Inorg. Chem.* **1995**, *34*, 3474–3476; e) M. Feist, S. Trojanov, E. Kemnitz, *Z. Anorg. Allg. Chem.* **1995**, *621*, 1775–1778; f) G. Aullón, D. Bellamy, L. Brammer, E. A. Bruton, A. G. Orpen, *Chem. Commun.* **1998**, 653–654; g) G. R. Lewis, A. G. Orpen, *Chem. Commun.* **1998**, 1873–1874; h) C. B. Aakeröy, T. A. Evans, K. R. Seddon, I. Pálkó, *New J. Chem.* **1999**, *23*, 145–152; i) M. Freytag, P. G. Jones, *Chem. Commun.* **2000**, 277–278; j) A. L. Gillon, G. R. Lewis, A. G. Orpen, S. Rotter, J. Starbuck, X.-M. Wang, Y. Rodriguez-Martin, C. Ruiz-Pérez, *J. Chem. Soc., Dalton Trans.* **2000**, 3897–3905; k) A. H. Mahmoudkhani, V. Langer, B. M. Casari, *Acta Crystallogr., Sect. E* **2001**, *57*, m393–m395; l) G. P. Schiemenz, *Z. Naturforsch.* **2007**, *62b*, 235–243.
- [12] P. B. Hitchcock, J. F. Nixon, J. Sinclair, *J. Organomet. Chem.* **1975**, *86*, C34–C36.
- [13] A. K. Chakravarty, F. A. Cotton, W. Schwotzer, *Inorg. Chim. Acta* **1984**, *84*, 179–185.
- [14] D. Carmichael, P. LeFloch, L. Ricard, F. Mathey, *Inorg. Chim. Acta* **1992**, *199*, 437–441.
- [15] B. J. Coe, T. J. Meyer, P. S. White, *Inorg. Chem.* **1995**, *34*, 593–602.
- [16] A. J. Ashe III, *J. Am. Chem. Soc.* **1971**, *93*, 3293–3295.
- [17] A. J. Ashe III, W. T. Chang, *J. Org. Chem.* **1979**, *44*, 1409–1413.
- [18] G. M. Sheldrick, *SHELXS-97, Program for the Solutions of Crystal Structures*, University of Göttingen, Germany, **1997**.
- [19] G. M. Sheldrick, *SHELXL-97, Program for the Refinement of Crystal Structures*, University of Göttingen, Germany, **1997**.
- [20] A. D. Becke, *Phys. Rev. A* **1988**, *38*, 3098–3100.
- [21] J. D. Perdew, *Phys. Rev. B* **1986**, *34*, 7406–7406.
- [22] J. D. Perdew, *Phys. Rev. B* **1986**, *33*, 8822–8824.
- [23] M. J. Frisch, G. W. Trucks, H. B. Schlegel, G. E. Scuseria, M. A. Robb, J. R. Cheeseman, J. A. Montgomery Jr, T. Vreven, K. N. Kudin, J. C. Burant, J. M. Millam, S. S. Iyengar, J. Tomasi, V. Barone, B. Mennucci, M. Cossi, G. Scalmani, N. Rega, G. A. Petersson, H. Nakatsuji, M. Hada, M. Ehara, K. Toyota, R. Fukuda, J. Hasegawa, M. Ishida, T. Nakajima, Y. Honda, O. Kitao, H. Nakai, M. Klene, X. Li, J. E. Knox, H. P. Hratchian, J. B. Cross, V. Bakken, C. Adamo, J. Jaramillo, R. Gomperts, R. E. Stratmann, O. Yazyev, A. J. Austin, R. Cammi, C. Pomelli, J. W. Ochterski, P. Y. Ayala, K. Morokuma, G. A. Voth, P. Salvador, J. J. Dannenberg, V. G. Zakrzewski, S. Dapprich, A. D. Daniels, M. C. Strain, O. Farkas, D. K. Malick, A. D. Rabuck, K. Raghavachari, J. B. Foresman, J. V. Ortiz, Q. Cui, A. G. Baboul, S. Clifford, J. Cioslowski, B. B. Stefanov, G. Liu, A. Liashenko, P. Piskorz, I. Komaromi, R. L. Martin, D. J. Fox, T. Keith, M. A. Al-Laham, C. Y. Peng, A. Nanayakkara, M. Challacombe, P. M. W. Gill, B. Johnson, W. Chen, M. W. Wong, C. Gonzalez, and J. A. Pople, *Gaussian 03, Revision D.01*, Gaussian, Inc., Wallingford CT, **2004**.
- [24] a) A. Schaefer, H. Horn, R. Ahlrichs, *J. Chem. Phys.* **1992**, *97*, 2571; b) D. Andrae, U. Häussermann, M. Dolg, H. Stoll, H. Preuss, *Theor. Chim. Acta* **1990**, *77*, 12.

Received: November 14, 2007
Published Online: June 13, 2008